



ELSEVIER

Biochimica et Biophysica Acta 1558 (2002) 34–44

BIOCHIMICA ET BIOPHYSICA ACTA

**BBA**[www.bba-direct.com](http://www.bba-direct.com)

# Dynorphin induced magnetic ordering in lipid bilayers as studied by $^{31}\text{P}$ NMR spectroscopy

Akira Naito \*, Takashi Nagao, Maki Obata, Yuriko Shindo, Manabu Okamoto, Shinya Yokoyama, Satoru Tuzi, Hazime Saitô <sup>1</sup>

*Department of Life Science, Himeji Institute of Technology, 3-2-1 Kouto, Kamigori, 678-1297 Hyogo, Japan*

Received 12 March 2001; received in revised form 11 September 2001; accepted 13 September 2001

## Abstract

Lipid bilayers of dimyristoyl phosphatidylcholine (DMPC) containing opioid peptide dynorphin A(1–17) are found to be spontaneously aligned to the applied magnetic field near at the phase transition temperature between the gel and liquid crystalline states ( $T_m = 24^\circ\text{C}$ ), as examined by  $^{31}\text{P}$  NMR spectroscopy. The specific interaction between the peptide and lipid bilayer leading to this property was also examined by optical microscopy, light scattering, and potassium ion-selective electrode, together with a comparative study on dynorphin A(1–13). A substantial change in the light scattering intensity was noted for DMPC containing dynorphin A(1–17) near at  $T_m$  but not for the system containing A(1–13). Besides, reversible change in morphology of bilayer, from small lipid particles to large vesicles, was observed by optical microscope at  $T_m$ . These results indicate that lysis and fusion of the lipid bilayers are induced by the presence of dynorphin A(1–17). It turned out that the bilayers are spontaneously aligned to the magnetic field above  $T_m$  in parallel with the bilayer surface, because a single  $^{31}\text{P}$  NMR signal appeared at the perpendicular position of the  $^{31}\text{P}$  chemical shift tensor. In contrast, no such magnetic ordering was noted for DMPC bilayers containing dynorphin A(1–13). It was proved that DMPC bilayer in the presence of dynorphin A(1–17) forms vesicles above  $T_m$ , because leakage of potassium ion from the lipid bilayers was observed by potassium ion-selective electrode after adding Triton X-100. It is concluded that DMPC bilayer consists of elongated vesicles with the long axis parallel to the magnetic field, together with the data of microscopic observation of cylindrical shape of the vesicles. Further, the long axis is found to be at least five times longer than the short axis of the elongated vesicles in view of simulated  $^{31}\text{P}$  NMR lineshape. © 2002 Elsevier Science B.V. All rights reserved.

**Keywords:** Magnetic ordering; Lipid bilayer; Dynorphin; DMPC;  $^{31}\text{P}$  NMR; Elongated vesicle

## 1. Introduction

Dynorphin A(1–17) is an endogeneous opioid heptadecapeptide,

Tyr-Gly-Gly-Phe-Leu-Arg-Arg-Ile-Arg-Pro-Lys-Leu-Lys-Trp-Asp-Asn-Gln(OH), which was originally isolated from porcine pituitary [1–3]. Dynorphin A(1–17) and A(1–13) bind to  $\kappa$ -opioid receptor with high affinity. The functional positions of dynorphin A(1–13) have been examined by means of enzymatic digestion [4]. It was found that Lys<sup>13</sup>, Lys<sup>11</sup> and Arg<sup>7</sup> residues play an essential role in the affinity of receptor binding. Subsequently, conformations of dynorphin A(1–17) and A(1–13) have been

\* Corresponding author. Present address: Faculty of Engineering, Yokohama National University, 79-5 Tokiwadai, Hodogaya-ku, Yokohama 240-8501, Japan. Fax: +81-45-339-4251.

*E-mail addresses:* [naito@ynu.ac.jp](mailto:naito@ynu.ac.jp) (A. Naito), [saito@sci.himeji-tech.ac.jp](mailto:saito@sci.himeji-tech.ac.jp) (H. Saitô).

<sup>1</sup> Also corresponding author. Fax: +81-791-58-0182

investigated by spectroscopic methods in solution [5–8], micelle [9], and lipid bilayers [10,11]. In aqueous solution, dynorphin A(1–13) takes an essentially unordered structure [5,6]. In contrast, dynorphin A(1–17) bound to micelles takes an  $\alpha$ -helical form from the residues Gly<sup>3</sup> through Pro<sup>10</sup> and contains a  $\beta$ -turn structure from residues Trp<sup>14</sup> through Gln<sup>17</sup> [9]. On the other hand, orientation of the  $\alpha$ -helical region of dynorphin A(1–13) was in parallel with the lipid bilayer normal [10]. It is most important to determine the conformation of dynorphin bound to the lipid bilayer, since it is thought that the peptide hormones encounter with lipid bilayer before interacting with the receptors [12,13]. Therefore, it is important to examine the manner of interaction of dynorphin with phospholipid bilayer by <sup>31</sup>P NMR spectroscopy as a model for naturally occurring cell membranes.

Much attention has been recently paid to magnetically oriented systems as a means to provide detailed information as to the conformation and dynamics of oriented molecules in biomembranes. Mechanically aligned lipid bilayers over glass plates have been extensively used to determine high resolution structure of membrane peptides [14–16]. Spontaneous magnetic orientation of lipid bilayer to the external magnetic field has been observed in pure phosphatidylcholine [17] and mixed phosphatidylcholine systems [18–22]. In these systems, partly extended vesicles are formed and the long axis is aligned parallel to the magnetic field. We have found that melittin-DMPC bilayer systems also show spontaneous magnetic alignment by forming elongated vesicle [23]. Recently, it has been reported that a mixture of phospholipid and detergent forms a bilayered micelle (bicelle) which exhibits magnetic orientation with the surface parallel to the magnetic field [24,25]. Although isolated diamagnetic molecules are not normally oriented spontaneously to the applied magnetic field because of a very small anisotropy of the magnetic susceptibility ( $\Delta\chi$ ), the assembled lipid molecules as in the elongated vesicles and bicelles give rise to a sufficiently large value of  $\Delta\chi$  to allow them to be aligned to the magnetic field. Because the sign of  $\Delta\chi$  in phospholipids is negative, the surface of the lipid bilayers is aligned parallel to the static magnetic field. Besides, it was demonstrated that the directions of the alignment can be altered by adding lanthanide

ions to the bilayers because of the large anisotropy of magnetic susceptibility in the presence of paramagnetic ions [26]. These magnetically oriented lipid bilayers can be used to examine the structures and orientations of membrane bound peptides or proteins [27,28]. In addition to the bicelles [29,30] and elongated vesicles which are spontaneously aligned to the magnetic field, the nematic phases of rod-shaped virus [31,32] and purple membranes [33] in buffer solutions have been utilized. In fact, this kind of alignment of biomolecules along the magnetic field has been also utilized as a constraint to refine the three-dimensional structure of globular proteins based on resulting residual dipolar and anisotropic chemical shift interactions [29].

We demonstrate here that the endogenous opioid peptide dynorphin exhibits an additional example to cause the lipid bilayers to be spontaneously oriented to the magnetic field, when incorporated into model membranes. In the case of melittin, magnetic alignment is caused above  $T_m$  by taking morphology of the elongated vesicle as a result of induced lysis and membrane fusion [23]. We found that the process of lysis and fusion is a prerequisite to allow the orientation of lipid bilayers to the magnetic field. It is emphasized that dynorphin-DMPC systems show a highly ordered bilayer alignment the same as that of bicelles and melittin-DMPC bilayers. Undoubtedly, this system provides an excellent means to examine the manner of lipid–protein or lipid–peptide interactions as in the case of bicelles [27].

## 2. Materials and methods

Dynorphin A(1–17) and A(1–13) were synthesized by means of Fmoc chemistry using an Applied Biosystems 431A peptide synthesizer. Crude peptides were purified using a Waters HPLC system with a BONDASPHERE C<sub>18</sub> reversed phase column. Peptide to DMPC molar ratios of 1:5, 1:10, 1:20, and 1:50 were dissolved in methanol and the solvent was completely removed in vacuo, followed by hydration with deionized (1:10) water and 20 mM Tris buffer containing 100 mM NaCl (1:5, 1:20, and 1:50). The hydrated sample was centrifuged to concentrate the lipid bilayers and final lipid contents were adjusted to 20% w/v. For the ion leaking experiment, 0.4 ml of a

lipid bilayer dispersion was prepared with buffer (20 mM Tris, 100 mM KCl, and pH 7.4) followed by adding 100 ml of Tris buffer containing 100 mM NaCl and 1 ml of 5% w/v Triton X-100 was added to the solution in drops to dissolve the lipid bilayers while keeping the temperature at 40°C and 5°C.

$^{31}\text{P}$  NMR spectra were recorded on a Chemagnetics CMX 400 NMR spectrometer with and without magic angle spinning under high power proton decoupling. The 90° pulse width of 6  $\mu\text{s}$  was used followed by the acquisition under the  $^1\text{H}$  decoupling field of 50 kHz. In the MAS experiments, 80  $\mu\text{l}$  of sample was placed in a 5 mm OD zirconia rotor and the top and bottom parts were completely sealed with a teflon cap using glue to prevent sample leakage. The spinning frequency was set to  $1500 \pm 2$  Hz using a spinning controller. The sample temperature was regulated using gas flow in the stator assembly.  $^{31}\text{P}$  chemical shift was referred to that of 85%  $\text{H}_3\text{PO}_4$ . Light scattering measurements were performed using a Shimadzu UV-2200 UV-VIS spectrophotometer equipped with a temperature control unit. Potassium ion-selective and reference electrodes (Horiba Ltd., Kyoto, Japan), and an ion meter (Horiba Ltd.) were used to measure the leakage of potassium ions from the vesicles by treating with Triton X-100. Microscope measurements were performed on a Nikon Optiphot2 microscope equipped with a Coolpix950 digital camera. Temperature was controlled by a temperature controlled stage for the microscope (TOKAI HIT, Shizuoka, Japan).

### 3. Results

Fig. 1 shows a plot of the intensity of light scattering of DMPC bilayer containing dynorphin A(1–17) versus temperature. When the bilayers were prepared by mixing DMPC with dynorphin A(1–17) with molar ratio of 10:1, followed by hydration with deionized water, the scattered intensity was decreased dramatically by lowering the temperature from 30 to 20°C (open circles). At 23°C, the scattered intensity was almost three orders of magnitude smaller than that at 30°C. The scattered intensity was increased again at 25°C as the temperature was raised. Apparently, the temperature at which the scattering intensity critically changes coincides with  $T_m$  ( $=24^\circ\text{C}$ ).

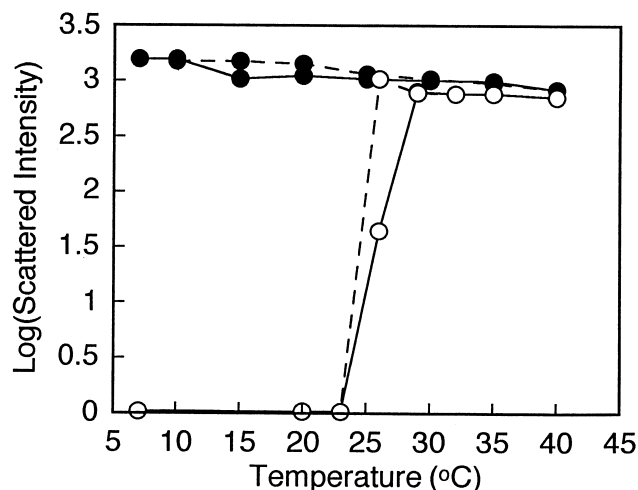


Fig. 1. Plots of the light scattered intensity at 480 nm against the temperature for the DMPC bilayers in the presence of dynorphin A(1–17).  $\circ$ : the peptide was added to this bilayer before hydration;  $\bullet$ : the peptide was added after hydration; solid line: raising the temperature; dashed line: lowering the temperature.

Although it takes 30 min to equilibrate the scattering intensity, lysis and fusion of lipid bilayer induced by dynorphin can occur reversibly by varying the temperature across  $T_m$ . In contrast, the scattering intensities of the bilayer did not change over a temperature range from 7 to 40°C (closed circles) as shown in Fig. 1, when dynorphin was added to hydrated DMPC bilayers after preparing multilamellar vesicles (MLV).

Fig. 2 shows the microscopic pictures of DMPC bilayer in the presence of dynorphin A(1–17). At 10°C, a few number of small vesicles undergoing Brownian motion were clearly visible in the transparent solution (Fig. 2A). The solution turned white to yield the small needle type patterns, when the temperature was raised to 20°C (Fig. 2B). After waiting for a half day at 30°C, the large vesicles with bending cylindrical shape appeared (Fig. 2C). When the temperature was lowered, the needle type patterns readily disappeared at 18°C and the solution became transparent. This microscope observation indicates that vesicles are formed at a temperature above 18°C which is lower than  $T_m$  and the vesicles are consequently lysed to small micelles below 18°C. It is also shown in Fig. 2 that DMPC vesicles containing dynorphin tend to aggregate each other to yield the strong light scattering.

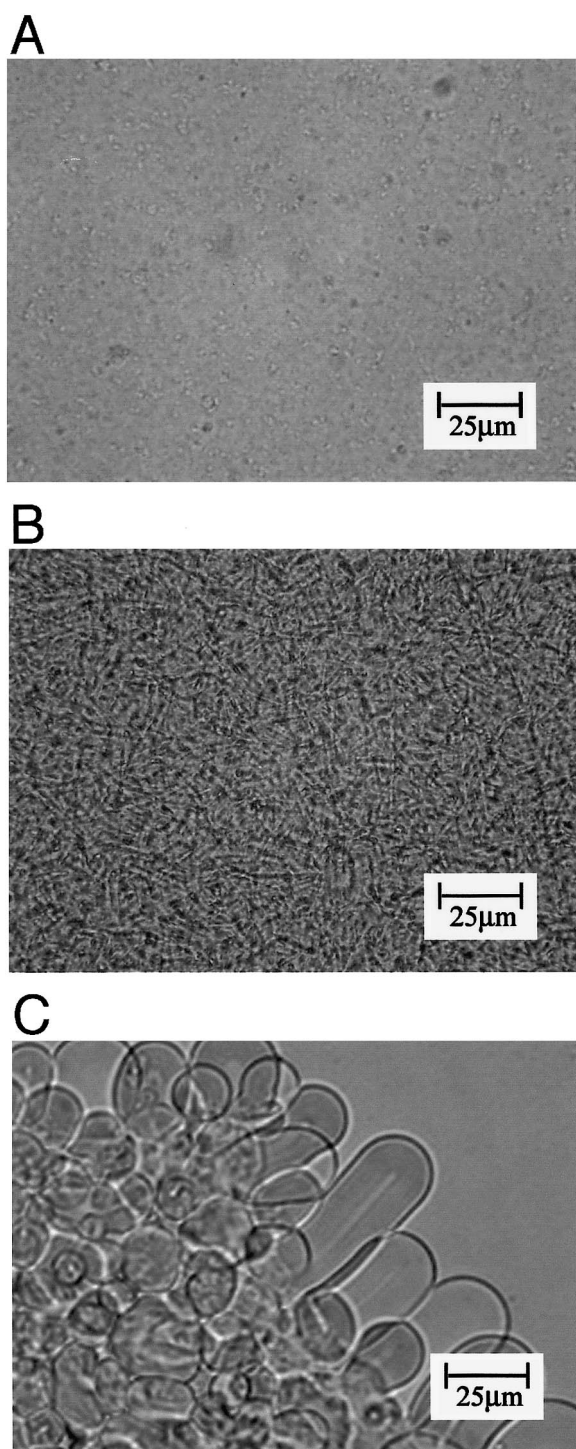


Fig. 2. Pictures of microscope for the DMPC bilayer containing dynorphin A(1–17) at 10°C (A), 20°C (B), and 30°C (C). Dynorphin to DMPC molar ratio is 1:10.

We have further investigated whether the vesicle are really formed or not above and below  $T_m$  of DMPC bilayer in the presence of dynorphin, as viewed from leakage of potassium ion from the lipid bilayers by a potassium ion-selective electrode. Fig. 3 illustrates the potassium leakage by adding 1 ml of 5% w/v Triton X-100 into the dynorphin-DMPC systems to dissolve the lipid in the buffer. It was clearly demonstrated that potassium ions leaked out from the bilayers immediately after adding a drop of Tri-

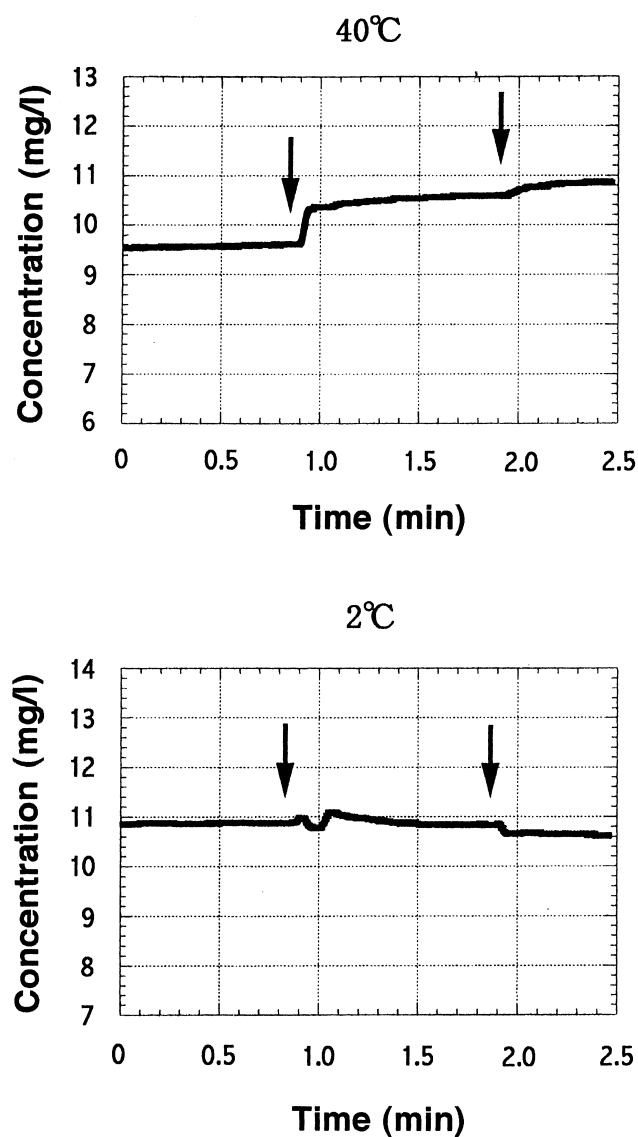


Fig. 3. Plot of potassium concentration measured by a potassium ion-selective electrode as a function of time at 40°C (top) and 0°C (bottom), respectively. 1 ml of 5% w/v Triton X-100 solution was added at the arrow positions.

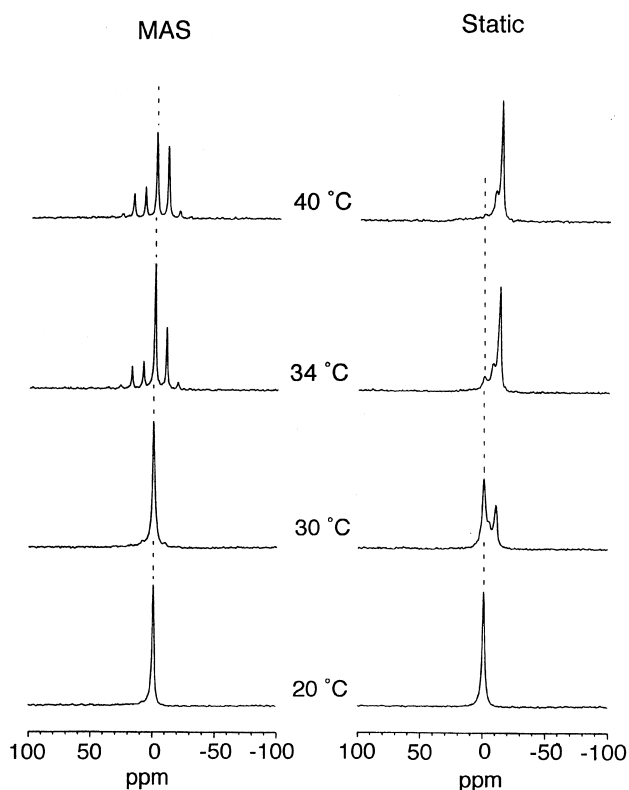


Fig. 4. Temperature variation of the  $^{31}\text{P}$  NMR spectra taken under the MAS (left panel) and static (right panel) conditions of the DMPC bilayer in the presence of dynorphin A(1–17) hydrated with deionized water. Dynorphin to DMPC molar ratio is 1:10. The  $^{31}\text{P}$  chemical shift values are referenced to the  $^{31}\text{P}$  NMR signal of concentrated  $\text{H}_3\text{PO}_4$  solution. Spinning frequency is 1500 Hz in the MAS experiment.

ton X-100 solution, when the temperature was raised above  $T_m$ . In contrast, potassium ions did not leak out from the bilayers when the temperature was below  $T_m$ . In other words, potassium ions were not trapped in the bilayers because vesicles were not formed below  $T_m$ . These results clearly indicate that the bilayer vesicles were formed above  $T_m$ , whereas discoidal bilayers or micelles were formed at a temperature below  $T_m$ .

To examine the interaction between DMPC bilayers and dynorphin,  $^{31}\text{P}$  NMR spectra of DMPC bilayers were recorded under the condition of magic angle spinning in the presence of dynorphin A(1–17) with molar ratio of 10:1, at various temperatures as illustrated in Fig. 4. Many sideband signals were observed in the  $^{31}\text{P}$  MAS NMR spectra due to a large chemical shift anisotropy as compared with the magic angle frequency (1.5 kHz) above 34°C (left panel

of Fig. 4). The presence of large chemical shift anisotropy is distinguished as far as the size of bilayer vesicles are sufficiently large. These sidebands, however, disappeared to yield the isotropic peak at 0 ppm, when the temperature was lowered to 20°C. Undoubtedly, the presence of this kind of the isotropic  $^{31}\text{P}$  NMR peak is characteristic of the presence of a small sized bilayer as referred to the  $^{31}\text{P}$  NMR signal of concentrated  $\text{H}_3\text{PO}_4$  solution. These results are consistent with the substantially decreased light scattering intensity as a result of lysis below 30°C.

The static  $^{31}\text{P}$  NMR signal of isotropic component is again resonated at 0 ppm at the same position with that of the MAS NMR experiment below 34°C (Fig. 4, right panel). In contrast, it is noteworthy that the  $^{31}\text{P}$  NMR signal was shifted upfield to  $-12$  ppm from the isotropic signal position at 34°C. This means that the bilayers are spontaneously aligned to the static magnetic field, as manifested from the peak position of the perpendicular component of the  $^{31}\text{P}$  chemical shift tensor of DMPC in the liquid crystalline phase [34]. In other words, the bilayer surface is aligned parallel to the static magnetic field. A similar manner of magnetic ordering of lipid bilayer along the magnetic field has been reported re-

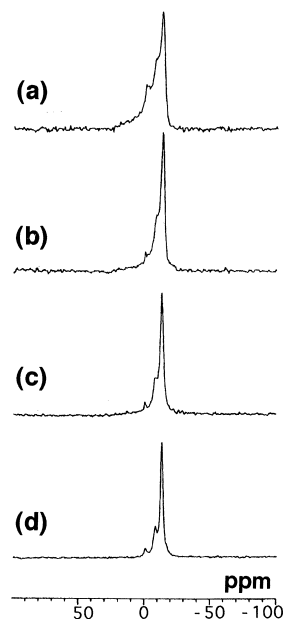


Fig. 5. Time course of the  $^{31}\text{P}$  NMR spectra of dynorphin A(1–17)-DMPC bilayer system after 6.7 min (a), 20 min (b), 33 min (c), and 12 h (d) from the stop of MAS at 36°C.

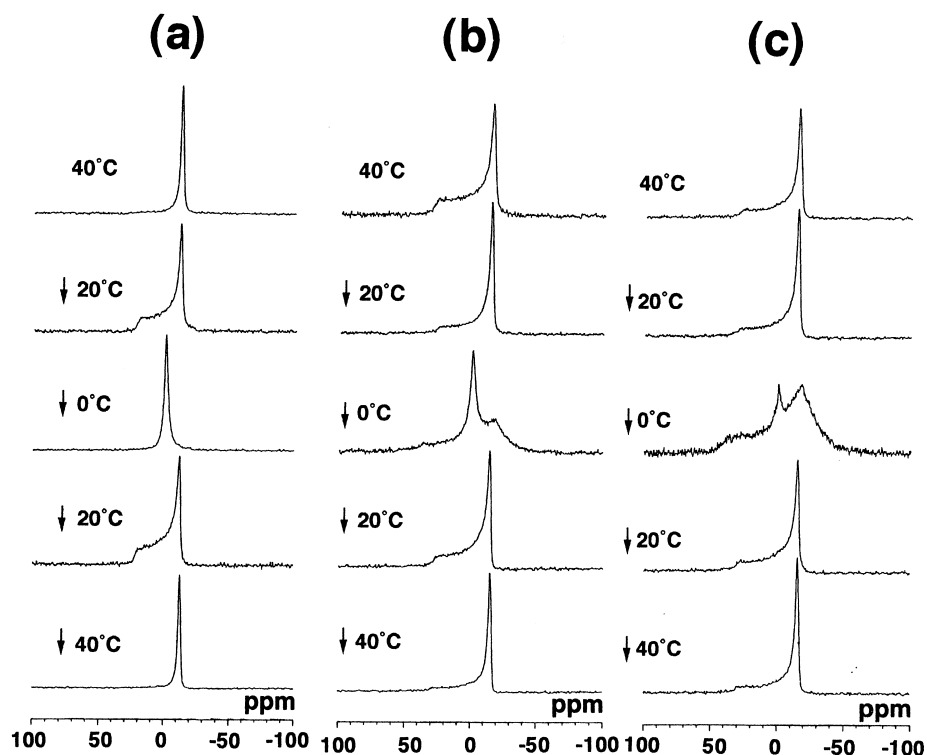


Fig. 6. Temperature variation of the  $^{31}\text{P}$  NMR spectra of DMPC dispersion in the presence of dynorphin A(1–17) hydrated with Tris buffer (pH 7.4). Dynorphin A(1–17) to DMPC molar ratios are 1:5 (a), 1:20 (b), and 1:50 (c).

cently in a mixed lipid system (DMPC/DHPC or CHAPSO mixture) to form the bicelles [24,25] and in a melittin-DMPC system to form the elongated vesicles [23]. In the case of bicelles containing DMPC and DHPC, two components of  $^{31}\text{P}$  NMR peaks are visible due to the presence of the two types of phosphate groups in DMPC of the bilayer part and DHPC of the edge part, when the bicelles are aligned to the magnetic field. It is emphasized that the absence of such minor component in the two  $^{31}\text{P}$  peaks arising from the edge part of a disc type bilayer does not appear in the present dynorphin A(1–17)-DMPC systems. This means that the bilayer system is entirely homogeneous in contrast to the case of the bicelle system. The presence of small peaks at  $-6$  ppm in the right panel of Fig. 4 is attributed to the lysophosphatidylcholine after hydrolysis of the acyl chain, because the pH value of the dispersion hydrated with deionized water is 3.0 at which hydrolysis reactions may occur.

This sort of magnetic ordering is disturbed by magic angle spinning [35,36] as manifested from the sideband pattern due to chemical shift anisotropy in

the  $^{31}\text{P}$  MAS NMR spectra above  $34^\circ\text{C}$ . Immediately after the MAS was stopped at  $36^\circ\text{C}$ , the anisotropic  $^{31}\text{P}$  NMR signals were gradually changed to the narrow component, indicating that magnetic alignment was gradually recovered (Fig. 5). It is noteworthy that approximately 30 min were required to be able to record the  $^{31}\text{P}$  NMR signals of the completely magnetically ordered state at  $36^\circ\text{C}$ . It takes even longer to recover the magnetic ordering at a higher temperature.

Fig. 6 shows the  $^{31}\text{P}$  NMR spectra of DMPC bilayer in the presence of dynorphin A(1–17) with molar ratios of 5:1, 20:1 and 50:1 hydrated with Tris buffer (pH 7.4). Apparently, the  $^{31}\text{P}$  powder pattern NMR spectra were recorded at a temperature around  $20^\circ\text{C}$ , in contrast to the case of Fig. 4. The isotropic narrow signal is present below  $T_m$ , for DMPC bilayer containing dynorphin A(1–17) with molar ratio of 5:1. The powder pattern  $^{31}\text{P}$  NMR spectrum was again visible below  $T_m$ . Above  $T_m$ , the narrow single line was seen at  $-12$  ppm which is resonated at higher field than that of isotropic signals above  $T_m$ . This result clearly indicates that the bilayers containing

dynorphin exhibit magnetic ordering with the bilayer surface parallel to the magnetic field. Interestingly, lysis was not completed even at 0°C, when DMPC to dynorphin was increased to the molar ratios of 20:1 and 50:1. In addition, the extent of magnetic ordering turned out to be not high enough as compared to the case of DMPC to dynorphin with molar ratio 5:1. It is also noticed that sufficient magnetic ordering is achieved when lysis and fusion were performed in the presence of the magnetic field. It is also notable that DMPC bilayer containing dynorphin A(1–17) hydrated with Tris buffer (pH 7.4) exhibits powder pattern  $^{31}\text{P}$  NMR spectra at 20°C, in contrast to the case of DMPC bilayers hydrated with deionized water (pH 3.0) (Fig. 4). This result indicates that the manner of interaction of dynorphin with DMPC bilayers depends on the pH. In addition, no signal was recognized at  $-6$  ppm due to the presence of lysophosphatidylcholine, because reaction rate of hydrolysis of phospholipids is considerably slow at pH 7.4.

Fig. 7 shows the  $^{31}\text{P}$  NMR spectra of DMPC bilayers in the presence of dynorphin A(1–13) with molar ratio of 5:1 hydrated with Tris buffer. Obviously, the  $^{31}\text{P}$  powder pattern NMR spectra were visible even if placed in the magnetic field at 40°C. This pattern was substantially broadened at 0°C. This powder pattern did not change to the single peak even after the temperature was raised to above  $T_m$ . It is interesting to note that complete magnetic ordering was not achieved in this system at a temperature above  $T_m$ , although the perpendicular component was substantially increased as compared with the parallel component. The broadened powder pattern due to the gel phase was seen at 0°C, indicating that lysis did not occur in this system. It is therefore important to conclude that the C-terminal four amino acid residues of dynorphin A(1–17) play a crucial role to cause the lysis and fusion to the lipid bilayers.

## 4. Discussion

### 4.1. Mechanism of the magnetic ordering of dynorphin-DMPC system

To understand the underlying mechanism of the magnetic ordering of the lipid bilayers, it seems to

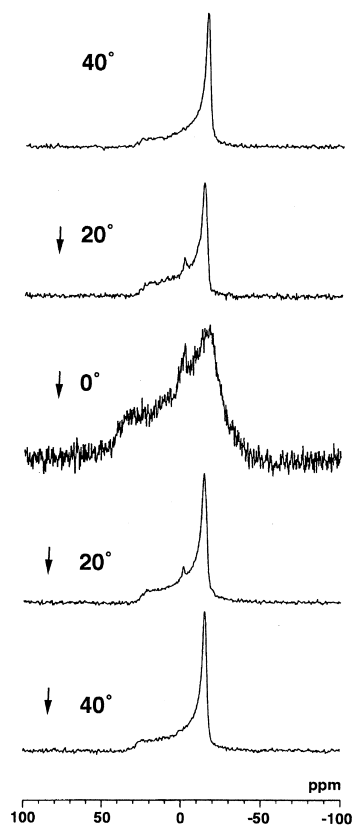


Fig. 7. Temperature variation of  $^{31}\text{P}$  NMR spectra of DMPC bilayer in the presence of dynorphin A(1–13) hydrated with Tris buffer (pH 7.4). Dynorphin to DMPC molar ratio is 1:5.

be important to clarify how their morphology is modified in the presence of dynorphin at a temperature around  $T_m$ . It was shown that the lysis of bilayers occurs below  $T_m$  to break down into small sized micelles or discoidal type of bilayers which show the isotropic  $^{31}\text{P}$  NMR signals. These small bilayer particles can be fused to grow into large vesicles above  $T_m$  and to show a large anisotropy in the  $^{31}\text{P}$  NMR spectra (Figs. 4 and 6). The formation of large vesicle was clearly proved by the leakage experiment of potassium ion. It is pointed out that the shape of the vesicle should be distorted to make the elongated vesicle as schematically drawn in Fig. 8, if this fusion process occurred in the presence of the magnetic field. This is proved by the fact that most surfaces of the lipid bilayers are parallel to the applied magnetic field, because the peak intensity corresponding to the perpendicular component of the  $^{31}\text{P}$  chemical shift tensor was substantially in-

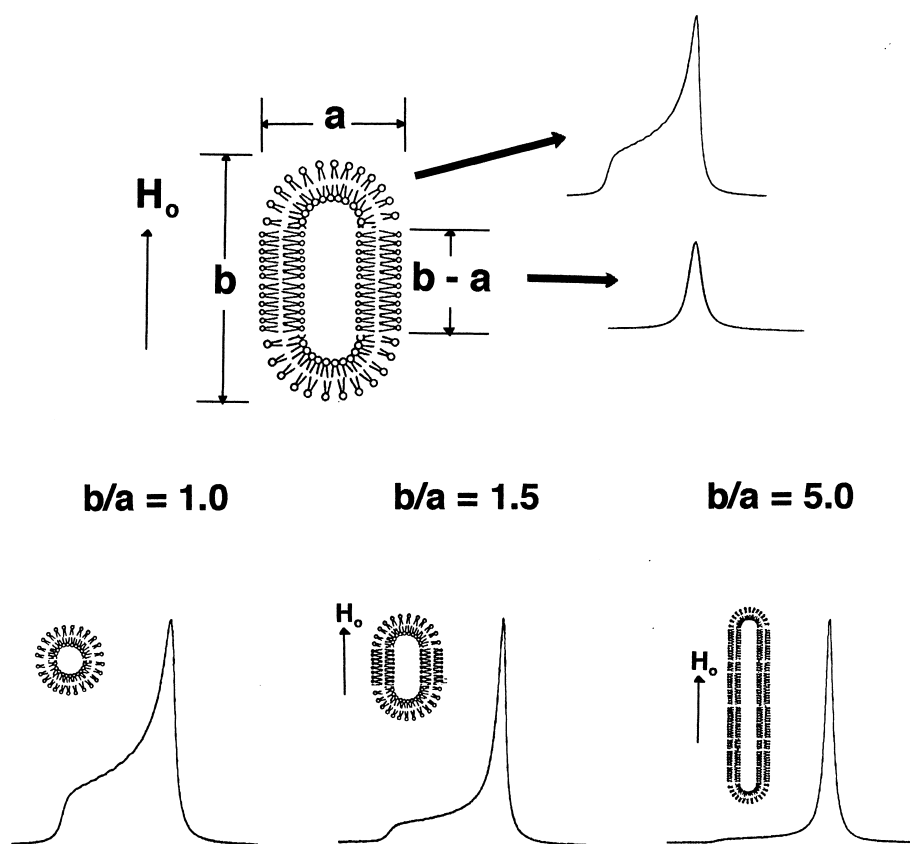


Fig. 8. Schematic representation of the elongated unilamellar vesicles in the magnetic field,  $H_0$ , and simulated  $^{31}\text{P}$  NMR spectra for a variety of elongated unilamellar vesicles. The  $a$  and  $b$  values denote the long and short axes of the elongated vesicles, respectively.

creased. Consequently, it is possible to consider that the elongated bilayer systems which possess positive diamagnetic anisotropy along the long axis of vesicle are formed [23]. The unique axis is then spontaneously aligned parallel to the magnetic field, as shown in Fig. 8, if the large elongated vesicle gains sufficient orientation energy. It appears that this alignment is caused by an assembly of lipids with small negative magnetic anisotropy in the bilayer along the acyl chain. In addition to expanding the size of the elongated vesicle, phase transition to the lyotropic liquid crystalline phase also appeared because the viscosity of the dynorphin A(1–17)-DMPC bilayer systems is increased at a temperature above  $T_m$ .

In the liquid crystalline state, the anisotropy of magnetic susceptibility can be characterized by  $\chi_{\parallel}$  and  $\chi_{\perp}$ . The magnetic susceptibility induces small magnetic moment in the lipid molecule and possesses

an orientation energy  $E$  in the presence of the magnetic field  $H_0$  as follows

$$E = -(1/2)H_0^2\{\chi_{\perp} + (\chi_{\parallel} - \chi_{\perp})\cos\theta\}, \quad (1)$$

where  $\theta$  is the angle between the  $\chi_{\parallel}$  and the magnetic field  $H_0$ . Therefore, the orientation energy of the lipid bilayer consisting of  $N$  number of lipid is expressed as

$$N\Delta E = -(1/2)N\Delta\chi H_0^2, \quad (2)$$

where  $\Delta E = E(\theta=0) - E(\theta=90)$  and  $\Delta\chi = \chi_{\parallel} - \chi_{\perp}$ . Thus a large number of molecules are required to possess enough magnetic anisotropy to be aligned to the static magnetic field. This consideration is supported by the fact that MLV of pure phospholipids are aligned to the magnetic field by forming an ellipsoidal shape [18,21]. In the case of phosphatidylcholine bilayer systems, MLV shows better magnetically



ordering than large unilamellar vesicle (LUV), partly because LUV is considerably flexible and hence the ellipsoidal shape cannot be well retained in LUV. In the case of the DMPC vesicles containing dynorphin, the magnetic ordering is also caused by the magnetic anisotropy of lipids rather than peptides, although the  $\alpha$ -helical peptides possess a positive magnetic anisotropy along the helical axis. However, it should be emphasized that the dynorphin-DMPC system forms a vesicle in the magnetic field and that dynorphin plays a crucial role to support the elongated shape of vesicle by strongly interacting with the lipid bilayers causing the strong magnetic alignment. We have also examined that another kind of peptide can be incorporated into the dynorphin-DMPC bilayer system keeping the magnetic orientation [37].

#### 4.2. Formation of elongated vesicles

It is emphasized that the elongated vesicles are formed for DMPC bilayer in the presence of dynorphin A(1–17), as discussed in the preceding section. It is also pointed out that this kind of the elongated vesicles was observed even in pure phospholipids when MLV is formed [17]. Indeed, the presence of the elongated vesicles is observed by phase contrast microscopy [18] and electron microscopy [21]. We consider a simple model to simulate the  $^{31}\text{P}$  NMR lineshape in terms of the elongated unilamellar vesicle. We first assume that the shape of vesicle is elongated in the presence of a certain length of the cylindrical part to the spherical unilamellar vesicle as shown in Fig. 8. Then, this view was confirmed by the fact that the  $^{31}\text{P}$  NMR signal of the cylindrical part of bilayer oriented parallel to the applied magnetic field yields the peak corresponding to the perpendicular position of the chemical shift tensor as indicated in Fig. 8. On the other hand, the spherical part will show the axially symmetric powder pattern at a temperature higher than  $T_m$ . In the simulation of the  $^{31}\text{P}$  NMR lineshape of the elongated vesicle in the magnetic field, we assume that the surface area reflects the number of phospholipids which give  $^{31}\text{P}$  NMR signals. Therefore, these patterns can be superimposed by mixing the ratio of surface and cylindrical area as shown in Fig. 8. When the short and the long axes of the elongated vesicles are denoted to be  $a$  and  $b$ , the relation between the area of the spher-

ical ( $S_s$ ) and cylindrical ( $S_c$ ) parts are given by

$$S_s = \pi a^2 \quad (3)$$

$$S_c = \pi a(b-a) \quad (4)$$

Under the condition when the total area is normalized by  $S_s + S_c = 1$ , the  $^{31}\text{P}$  NMR signal  $F$  is given by

$$F = F_{\text{pow}}(a/b) + F_{\perp}(1-a/b) \quad (5)$$

where  $F_{\text{pow}}$  and  $F_{\perp}$  denote the  $^{31}\text{P}$  NMR signals of spherical and cylindrical parts, respectively. It is of interest to point out that even in a small distortion from the sphere such as  $b/a = 1.5$ , a substantial building up of the perpendicular component in the powder pattern was seen as shown in Fig. 8. It turned out from the simulated results that the long axis is at least five times longer than the diameter of cylindrical rod of the elongated vesicle obtained in this experiment for dynorphin A(1–17)-DMPC bilayer systems. Therefore, most of the lipid bilayers in the elongated vesicles are considered to be magnetically oriented with the bilayer surface parallel to the magnetic field.

#### 4.3. Structural aspect of the interaction between dynorphin and membrane

In the structural point of view, it is reported that the N-terminus region forms the  $\alpha$ -helix which is inserted into the lipid bilayers as manifested from infrared attenuated total reflection (IR-ATR) spectroscopy [10] and  $^{13}\text{C}$  chemical shifts of [ $1\text{-}^{13}\text{C}$ ]Gly<sup>3</sup>, Phe<sup>4</sup>-labeled dynorphin (manuscript in preparation) with reference to the conformation dependent displacements of peaks [38]. Although both dynorphin preparations A(1–13) and A(1–17) form the  $\alpha$ -helical structure in the N-terminus, only dynorphin A(1–17) shows the strong lysis and fusion activity as already described. This fact indicates that the C-terminus region rather than the N-terminus region plays an important role to cause lysis and fusion, and hence magnetic ordering. It is emphasized that these portions may play a role in selecting the type of the opioid receptors as an *address* domain [4]. It is of interest to point out that the Trp residue is considered to be located at the membrane surface, because the fluorescence quenching experiment indicated the Trp residue was inserted into the membrane [9]. This

fact indicates that the Trp residue plays an important role for interaction with the membrane in the case of dynorphin A(1–17)-DMPC systems. On the other hand, dynorphin A(1–13) does not possess the Trp residue, and hence the dynorphin A(1–13)-DMPC bilayer did not show magnetic orientation. It is reported that the N-terminal region is inserted in the membrane, although the C-terminal region is located in the surface area [10]. It is likely that this insertion of the N-terminal may not give a strong perturbation to the membrane surface. However the interaction of the C-terminal region may play an important role in reducing the membrane surface pressure to cause fusion and lysis activities. In other words, binding of dynorphin A(1–17) with lipid bilayers is stronger than that of dynorphin A(1–13).

It is also observed that the interaction of dynorphin with bilayers in the dynorphin A(1–17)-DMPC system hydrated with deionized water is different from that hydrated with Tris buffer. Because the pH of the dynorphin A(1–17)-DMPC bilayer system hydrated with deionized water is 3.0, a part of phosphate group is protonated and negative charge is lost. Consequently, the electrostatic interaction of membrane surface with basic residues of dynorphin becomes weak, resulting in the different extent of lysis and fusion activities.

A similar process of lysis and fusion has been observed for bilayers containing melittin [23,39,40] and glucagons [41]. In the case of the melittin-DMPC system, the change of scattering intensities is much smaller when the temperature was varied across  $T_m$  [38]. This is because the vesicles in melittin-DMPC do not aggregate each other. It is found that the  $\alpha$ -helix of melittin shows the transbilayer orientation and the N- and C-terminal helix rods are tilting  $30^\circ$  and  $10^\circ$  from the average axis, respectively [23]. It has been reported for melittin-DMPC systems that small unilamellar vesicles are formed when the temperature was raised above  $T_m$  and the discoidal bilayers surrounded by peptides are formed at a temperature below  $T_m$  as viewed by electron microscope [39]. However we have observed the giant vesicles in melittin-DMPC bilayer systems above  $T_m$  [23]. In contrast to the case of melittin, the scattering intensity was substantially increased for DMPC bilayer containing glucagon when the temperature is lowered

from a higher temperature to  $T_m$ . It is reported that glucagons interact with lipids above and below  $T_m$ . Above  $T_m$ , the rate of vesicle aggregation is increased and below the  $T_m$ , glucagons form a stable complex with DMPC vesicles and rearrange to disk-shaped particles [36]. In the case of dynorphin-DMPC systems, it was essential that DMPC and dynorphin are mixed together before hydration in order to exhibit prominent lysis and bilayer fusion.

Because melittin is known to have lytic activity, it is natural to examine the property of lysis and fusion of lipid bilayers under the physiological point of view. On the other hand, dynorphin binds to a  $\kappa$ -opioid receptor in the cell membrane with high affinity [13]. However, it has not yet been reported that dynorphin has hemolytic activity. To the best of our knowledge, this is the first report that dynorphin induces lysis and fusion to lipid bilayers under high peptide to lipid ratio as in the present condition and this property is essential to induce high magnetic ordering.

#### 4.4. Conclusions

It is clearly demonstrated that dynorphin A(1–17) strongly interacts with lipid bilayers to cause fusion and lysis across  $T_m$  and results in subsequent high magnetic ordering at a temperature above  $T_m$ . We have shown that the elongated vesicles are formed in dynorphin A(1–17)-DMPC systems with the long axis parallel to the magnetic field, when the bilayers are placed in the high magnetic field. Because the proportion of the powder pattern in  $^{31}\text{P}$  NMR spectra is very low, the long axis is much longer than the short axis in the elongated vesicles of dynorphin A(1–17)-DMPC bilayers. On the other hand, the dynorphin A(1–13)-DMPC system did not exhibit magnetic ordering. This highly oriented DMPC bilayer containing dynorphin A(1–17) can be used to study the conformation of membrane proteins and peptides, as a simple spontaneously aligned system to the applied magnetic field, instead of a mechanically oriented system using glass plate and bicelle type membranes. We have also demonstrated that this system can be served as a better mimic of natural cell membrane, as this vesicle is fully hydrated and possesses a small curvature.

## Acknowledgements

This work was supported in part by a Grant-in-Aid from the Ministry of Education, Science, Sports and Culture of Japan.

## References

- [1] A. Goldstein, S. Tachibana, L.I. Lowney, M. Hunkapiller, L. Hood, *Proc. Natl. Acad. Sci. USA* 76 (1979) 6666–6670.
- [2] A. Goldstein, W. Fischli, L.I. Lowney, M. Hunkapiller, L. Hood, *Proc. Natl. Acad. Sci. USA* 78 (1981) 7219–7223.
- [3] S. Tachibana, K. Araki, S. Ohya, S. Yoshida, *Nature* 295 (1982) 339–341.
- [4] C. Chavkin, A. Goldstein, *Proc. Natl. Acad. Sci. USA* 78 (1981) 6543–6547.
- [5] V. Renugopalakrishnan, R.S. Rapaka, S.-G. Huang, S. Moore, T.B. Hutson, *Biochem. Biophys. Res. Commun.* 151 (1988) 1220–1225.
- [6] W.K. Surewicz, H.H. Mantsch, *J. Mol. Struct.* 214 (1989) 143–147.
- [7] C.R.D. Lancaster, K. Mishra, D.W. Hughes, S.A. St.-Pierre, A.A. Bothner-By, R.M. Epand, *Biochemistry* 30 (1991) 4715–4726.
- [8] J.W. Taylor, *Biochemistry* 29 (1990) 5364–5373.
- [9] M.R. Tessmer, D.A. Kallick, *Biochemistry* 36 (1997) 1971–1981.
- [10] D. Erne, D.F. Sargent, R. Schwyzer, *Biochemistry* 24 (1985) 4261–4263.
- [11] D.R. Alford, V. Renugopalakrishnan, *Duzgunes Int. J. Pept. Protein Res.* 47 (1996) 84–90.
- [12] L. Moroder, R. Romano, W. Guba, D.F. Mierke, H. Kessler, C. Delporte, J. Winand, J. Christophe, *Biochemistry* 32 (1993) 13551–13559.
- [13] D.F. Sargent, R. Schwyzer, *Proc. Natl. Acad. Sci. USA* 83 (1986) 5774–5778.
- [14] B.A. Cornell, F. Separovic, A.J. Baldassi, R. Smith, *Biophys. J.* 53 (1988) 67–76.
- [15] R.R. Ketchum, W. Hu, T.A. Cross, *Science* 261 (1993) 1457–1460.
- [16] F.M. Marassi, A. Ramamoorthy, S.J. Opella, *Proc. Natl. Acad. Sci. USA* 94 (1997) 8551–8556.
- [17] X. Qin, P.A. Miran, C. Pidgeon, *Biochim. Biophys. Acta* 1147 (1993) 59–72.
- [18] F. Scholz, E. Boroske, W. Helfrich, *Biophys. J.* 45 (1984) 589–592.
- [19] J. Seelig, F. Borle, T.A. Cross, *Biochim. Biophys. Acta* 814 (1984) 195–198.
- [20] J.B. Speyer, P.K. Sripada, S.K. Das Gupta, G.G. Shipley, R.G. Griffin, *Biophys. J.* 51 (1987) 687–691.
- [21] T. Brumm, A. Möps, C. Dolainsky, S. Bruckner, T.M. Bayerl, *Biophys. J.* 61 (1992) 1018–1024.
- [22] T. Pott, E.J. Dufourc, *Biophys. J.* 68 (1995) 965–977.
- [23] A. Naito, T. Nagao, K. Norisada, T. Mizuno, S. Tuzi, H. Saitô, *Biophys. J.* 78 (2000) 2405–2417.
- [24] C.R. Sanders II, J.H. Prestegard, *Biophys. J.* 58 (1990) 447–460.
- [25] C.R. Sanders II, J.P. Schwonek, *Biochemistry* 31 (1992) 8898–8905.
- [26] R.S. Prosser, S.A. Hunt, J.A. DiNatale, R.R. Vold, *J. Am. Chem. Soc.* 118 (1996) 269–270.
- [27] C.R. Sanders II, G.C. Landis, *Biochemistry* 34 (1995) 4030–4040.
- [28] K.P. Howard, S.J. Opella, *J. Magn. Reson.* 112B (1996) 91–94.
- [29] N. Tjandra, A. Bax, *Science* 278 (1997) 1111–1114.
- [30] M. Ottiger, A. Bax, *J. Biomol. NMR* 12 (1998) 361–372.
- [31] G.M. Clore, M.R. Starich, A.M. Gronenborn, *J. Am. Chem. Soc.* 120 (1998) 10571–10572.
- [32] M.R. Hansen, M. Rance, A. Pardi, *J. Am. Chem. Soc.* 120 (1998) 11210–11211.
- [33] B.W. Koenig, J.-S. Hu, M. Ottiger, S. Bose, R.W. Hendler, A. Bax, *J. Am. Chem. Soc.* 121 (1999) 1385–1386.
- [34] I.C.P. Smith, I.H. Ekiel, in: D.G. Gorenstein (Ed.), *Phosphorus-31 NMR: Principles and Application*, Ch. 15, Academic Press, New York, 1984.
- [35] J. Courtieu, D.W. Alderman, D.M. Grant, J.P. Bayles, *J. Chem. Phys.* 77 (1982) 723–730.
- [36] B.M. Fung, M. Gangoda, *J. Chem. Phys.* 83 (1985) 3285–3289.
- [37] S. Kimura, A. Naito, S. Tuzi, H. Saitô, *Biopolymers* 63 (2001) in press.
- [38] H. Saitô, S. Tuzi, A. Naito, *Annu. Rep. NMR Spectrosc.* 36 (1998) 79–121.
- [39] J. Dufourcq, J.-F. Faucon, G. Fourche, J.-L. Dasseux, M.L. Maire, T. Gulik-Krzywicki, *Biochim. Biophys. Acta* 859 (1986) 33–48.
- [40] C.E. Dempsey, B. Sternberg, *Biochim. Biophys. Acta* 1061 (1991) 175–184.
- [41] R.M. Epand, *Biochim. Biophys. Acta* 513 (1978) 185–197.